Progress In Electromagnetics Research C, Vol. 116, 65–80, 2021

Multiband Circularly Polarized Microstrip Patch Antenna with Minkowski Fractal Slot for Wireless Communications

Vijayankutty R. Remya[1], Manju Abraham[2], Ambalath R. Parvathy[3], and Thomaskutty Mathew[4, *]

Abstract—A multiband circularly polarized microstrip patch antenna including a Minkowski fractal slot for wireless communication applications in the frequency bands 1.39 GHz, 2.45 GHz (WLAN band), 3.48 GHz (Mobile Wi-Max), 5.8 GHz (U-NII high-band), and 6.29 GHz has been proposed. The proposed antenna consists of two substrates mounted on top of the ground plane. The antenna has been fed with a 50 Ω microstripline which is etched on top of the lower substrate. The second iteration Minkowski fractal slot is etched on a truncated square patch which is on top of the upper substrate. The substrate has a size of 80 mm × 82 mm × 1.6 mm. The measured results show that the proposed antenna could excite for five resonant bands of 1.35 GHz, 2.45 GHz, 3.5 GHz, 5.8 GHz, and 6.25 GHz, and has reflection coefficients of −15 dB for 1.35 GHz, −16 dB for 2.45 GHz, −22 dB for 3.5 GHz, −23 dB for 5.8 GHz, and −13 dB for 6.25 GHz as well as an axial ratio bandwidth of 3.42 GHz–3.47 GHz. The maximum gains of the antenna are 5.92 dBi for 1.39 GHz, 6.15 dBi for 2.45 GHz, 8.36 dBi for 3.48 GHz, 9.64 dBi for 5.8 GHz, and 6.69 dBi for 6.29 GHz. The simulations and optimizations have been carried through Computer Simulation Technology Microwave Studio (CST-MWS) software.

1. INTRODUCTION

Due to the low profile, conformability to planar, and non-planar surfaces, simple and inexpensive manufacture using modern printed-circuit technology, microstrip antennas are widely used in communication technology. In microstrip patch antennas radiating elements and feed lines are usually photoetched on dielectric substrates [1]. Slot-loaded patch antennas are found in various works for dual-band operations [2–4]. Multiple slits made on a rectangular patch are used for multiband operation in [5]. Loading slots and slits into the patch lowers the fundamental frequency and achieves multi-band operation. A frequency reconfigurable coplanar waveguide (CPW)-fed antenna [6] was reported by connecting different serpentine stubs by using PIN diodes. A substrate integrated waveguide based self trip plexing antenna for WiMAX, WLAN, and 5G was presented in [7]. Meandering of the excited surface current paths in the radiating patch takes place by loading slots and slits on radiating patch [3].

Circular polarization yields various advantages like flexibility in the orientation of the transmitter and receiver in wireless communication. It increases the impedance, efficiency, and axial ratio bandwidth of RF systems. Two orthogonal linearly polarized modes with equal amplitude and 90° phase difference can achieve circular polarization. Asymmetrical fractal boundary is reported for circular polarization [8]. Using truncated patches with slits is reported for a considerable amount of size reduction and circular polarization [9]. Four different circularly polarized microstrip antenna structures with cross slots on

Received 25 July 2021, Accepted 28 September 2021, Scheduled 10 October 2021

* Corresponding author: Thomaskutty Mathew (tmathew@gitam.edu).

[1] Department of Electronics, School of Technology and Applied Sciences, Mahatma Gandhi University, Regional center, Edappally, Kerala, India. [2] Department of Electronics, BPC College, Piravom, Kerala, India. [3] Division of Electronics & Communication Engineering, Cochin University College of Engineering, Kuttanad, CUSAT, Alappuzha, Kerala, India. [4] Department of Physics, School of Sciences, GITAM Deemed to be University, Bengaluru Campus, Nagadenahalli, Bengaluru Rural, Karnataka, India.

the patch were proposed in [10]. An irregular slot with a stair shaped edge and L-shaped feed line was presented in [11]. A stair shaped edge improved the circular polarization of the antenna. Omnidirectional circularly polarized antenna with single feed for 2.4 GHz WLAN applications was presented in [12]. An antenna with improved impedance matching and bandwidth using inverted T-shaped slots and L-shaped stubs in the ground plane with truncated corners was designed by Bhatia and Sharma [13]. In the proposed antenna for achieving circular polarization truncated patch was employed. A truncated square patch provides perturbation to generate circular polarization.

Fractal-shaped antennas have attracted a lot of attention in wireless communication. A single antenna can operate at many frequency bands which is the favoring circumstance of using a multiband antenna. Applying fractal shapes into antenna geometry is one of the methods of constructing a multiband antenna. Recently, a few works have been reported in slot antennas to achieve dual-band using fractal geometries [14–16]. A rhombic patch monopole antenna with Minkowski fractal offering multiband was introduced in [17]. In [18], the second iteration Koch fractal curve applied on one of the side lengths of a rectangular slot antenna has been reported for multiband wireless communication applications. Koch-shaped fractal defects on the patch surface for size reduction of microstrip antenna have been reported in [19]. A fractal Jerusalem cross slot antenna for circular polarization was presented in [20]. A circularly polarized single-feed microstrip slot antenna based on fractal offers size reduction of the patch has been reported in [21]. In [22], Sierpinski-based fractal geometry on the patch with meandered transmission line is utilized for L-band applications. The inserted Minkowski fractal slot in the proposed antenna can result in the meandering of the excited surface current path which lowers the resonant frequency in each iteration. In this paper, a truncated square patch antenna loaded with Minkowski fractal slot with proximity coupled feeding technique is present.

2. REALIZATION OF MINKOWSKI STRUCTURE

Benoit B. Mandelbrot was the first to use the term fractal [23]. Fractal geometries are generated using an iteration process that guides to self-similar structures [24–25]. In the proposed antenna, a Minkowski island fractal structure is utilized. The basic geometry of the generation process is referred as initiator which in Minkowski island is a Euclidean square. Each of the four straight sides in this square is replaced by a generator. The first two generated iterations are shown in Figure 1.

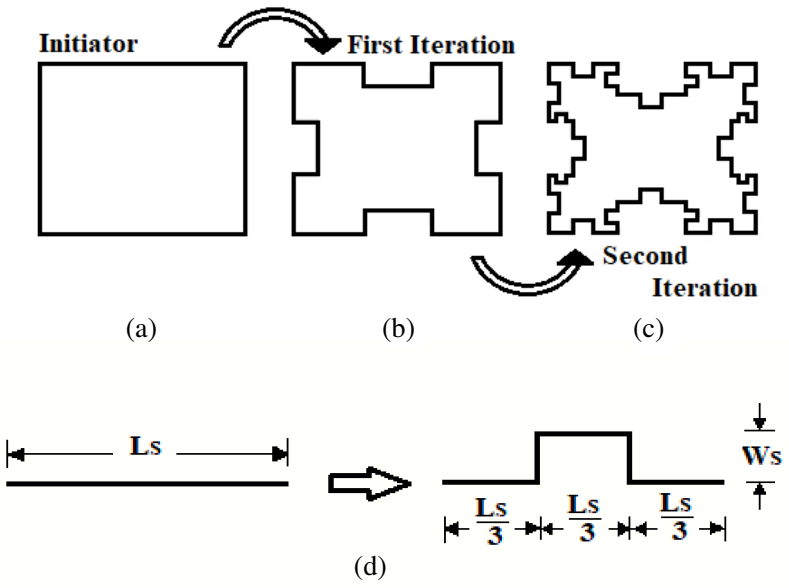

Figure 1. The generation of the Minkowski fractal. (a) The zero iteration. (b) First iteration. (c) Second iteration. (d) Initial generator.

3. ANTENNA DESIGN

In this antenna, two dielectric substrates are used such that a $50\,\Omega$ microstrip feedline is between two substrates. A truncated radiating patch with Minkowski fractal slot and a cross structure at the center is made on top of the upper substrate (substrate 2). The patch is made of perfect electrical conductor (PEC), and substrates are made of FR-4 with a dielectric constant of 4.4 and thickness of 1.6 mm. The lower substrate (substrate 1) is made on the top of the ground plane. The size of the ground plane and substrate is $80 \times 84\,\text{mm}^2$. A microstripline, with a length about 6 mm and width of 3.3 mm is etched on top of the lower substrate. Figure 2 shows the geometry of the proposed Minkowski slotted truncated patch antenna.

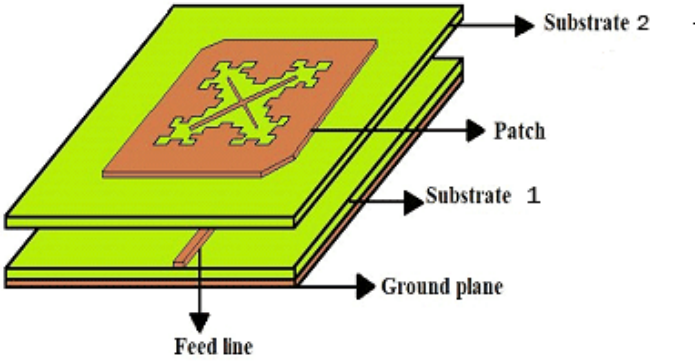

Figure 2. The geometry of the Minkowski slotted truncated patch antenna.

On each end, the dimensions of the patch along the length have been extended by a length ΔL because of the fringing effect and the relation as given in Equation (1). To compute the physical dimension of a rectangular patch antenna, the length and width expressions are given below [1].

$$\frac{\Delta L}{h} = 0.412 \frac{(\varepsilon_{ref} + 0.3)\left(\frac{W}{h} + 0.264\right)}{(\varepsilon_{ref} - 0.258)\left(\frac{W}{h} + 0.8\right)} \tag{1}$$

where h is the height of the substrate, $\frac{W}{h}$ the width to height ratio, and ε_{ref} an effective dielectric constant.

$$\varepsilon_{ref} = \frac{\varepsilon_r + 1}{2} + \frac{\varepsilon_r - 1}{2}\left[1 + 12\frac{h}{W}\right]^{-1/2}; \quad \frac{W}{h} > 1 \tag{2}$$

Physical width,

$$W = \frac{c}{2f_r}\sqrt{\frac{2}{\varepsilon_r + 1}}, \tag{3}$$

where c is the free space velocity of light, and ε_r is the dielectric constant of the substrate.

Physical length,

$$L = \frac{1}{2fr\sqrt{\varepsilon_{ref}}\sqrt{\mu_0\varepsilon_0}} - 2\Delta L \tag{4}$$

Figure 3 shows the dimensions of the proposed truncated patch antenna with the second iteration Minkowski slot. The optimized parameter values of the proposed antenna are given in Table 1.

4. PARAMETRIC STUDY

In this work, the improvement of antenna performance for wireless communication applications is done through optimization with simulation software CST microwave studio. Figure 4(a) shows the generator

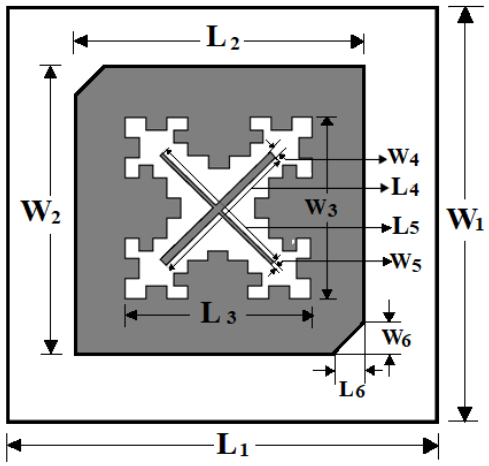

Figure 3. The dimensions of the proposed second iteration Minkowski slotted truncated patch antenna.

Table 1. Optimized parameter values of the proposed antenna.

Parameters	L_1	W_1	L_2	W_2	L_3	W_3	L_4	W_4	L_5	W_5	L_6	W_6
Value (mm)	84	80	42	40	21	20	8	0.5	7	0.2	5	5

slot, and Figures 4(b) and (c) show the first and second Minkowski fractal iteration levels. Figure 5 shows the frequency vs reflection coefficient of different iteration levels. Table 2 shows resonant frequencies for each iteration and the corresponding reflection coefficient and gain. By changing the iteration levels of fractal structure, it can be stated that there are some different characteristics in terms of reflection

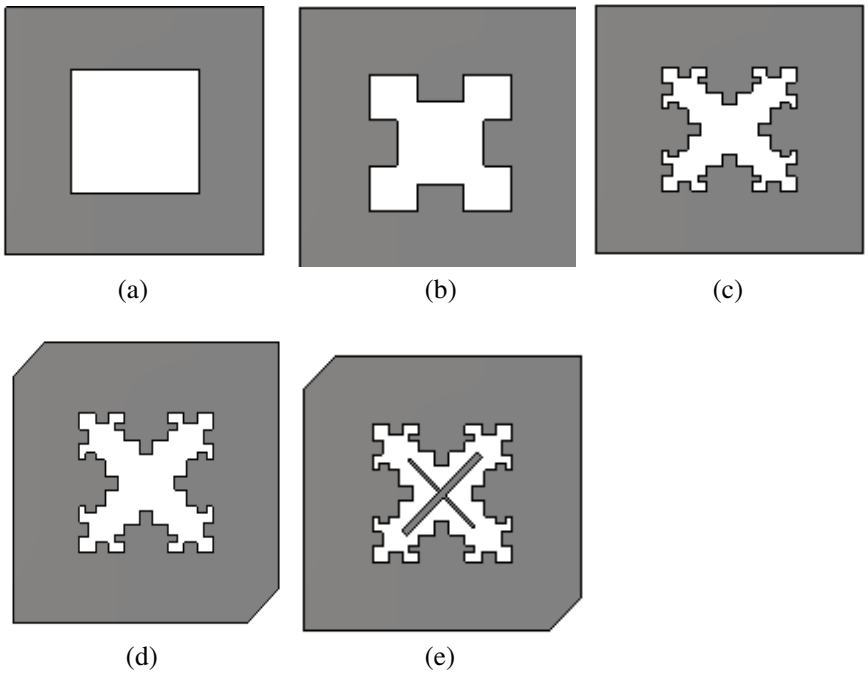

Figure 4. The evolution of the design stages of different prototypes of the proposed antenna. (a) Generator slot in the patch. (b) First iteration. (c) Second iteration. (d) Applying truncation. (e) Proposed prototype of antenna patch.

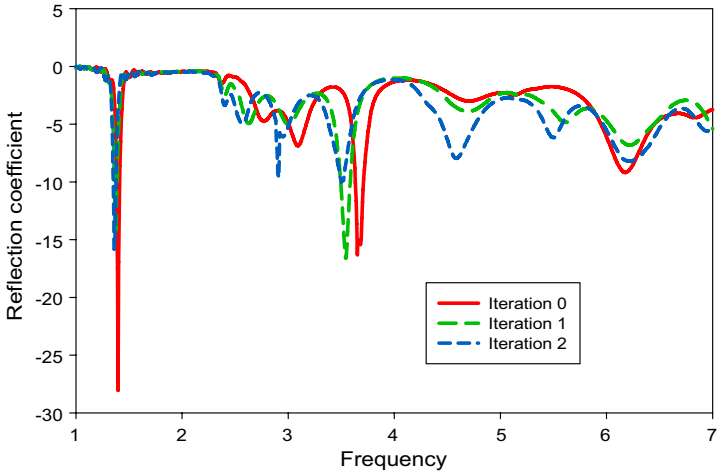

Figure 5. Frequency vs reflection coefficient of different iteration levels.

Table 2. Characteristics of different iteration levels.

PARAMETER	RESULTS						
	Iteration 0 (generator slot)		Iteration 1		Iteration 2		
Resonant frequency (GHz)	1.396	3.67	1.372	3.54	1.36	2.9	3.5
Gain (dBi)	5.92	6.06	5.89	8.28	5.86	5.59	8.39
Reflection coefficient (dB)	−28	−26	−14	−16	−15.8	−9.6	−10

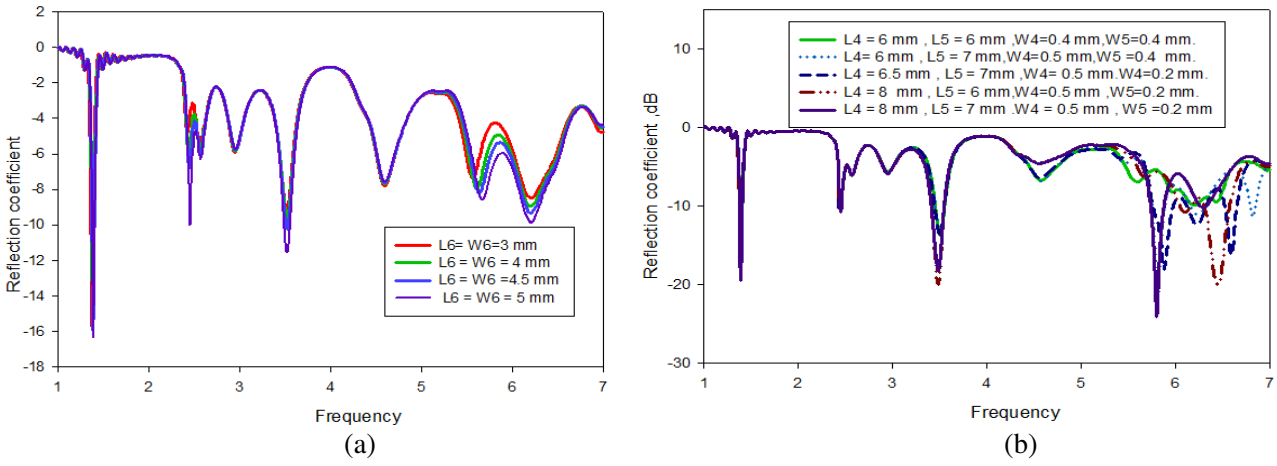

Figure 6. Parametric study results for different parameter values. (a) Effect of cutting length and width, L_6 and W_6. (b) Cross structure dimensions (L_4, L_5, W_4, W_5).

coefficient, return loss, and gain as shown in Table 2.

For more optimization, the patch was made truncated, and a cross structure was inserted at the centre as shown in Figures 4(d) and (e). The effect of parameters L_6 and W_6 of truncation on the

reflection coefficient is as shown in Figure 6(a). It is observed that with $L_6 = W_6 = 5\,\text{mm}$ the antenna exhibits good reflection coefficient. The effect of parameters L_4, L_5, W_4, and W_5 of cross structure on the reflection coefficient of the proposed antenna is as shown in Figure 6(b). From the analysis it is observed that the cross structure at the centre of patch controls the two higher resonant frequencies 5.8 GHz and 6.29 GHz. By adding a cross structure the two higher resonant frequencies change without changing the three lower resonant frequencies. It can be seen that at $L_4 = 8\,\text{mm}$, $L_5 = 7\,\text{mm}$, $W_4 = 0.5\,\text{mm}$, and $W_5 = 0.2\,\text{mm}$, the antenna exhibits more improved performance.

Asymmetry in the structure is made by truncation and unequal lengths and widths of cross structure which enhances circular polarisation in the 3.46 GHz of resonant frequency. Figure 7 shows the comparison of reflection coefficients with and without the cross structure at the centre.

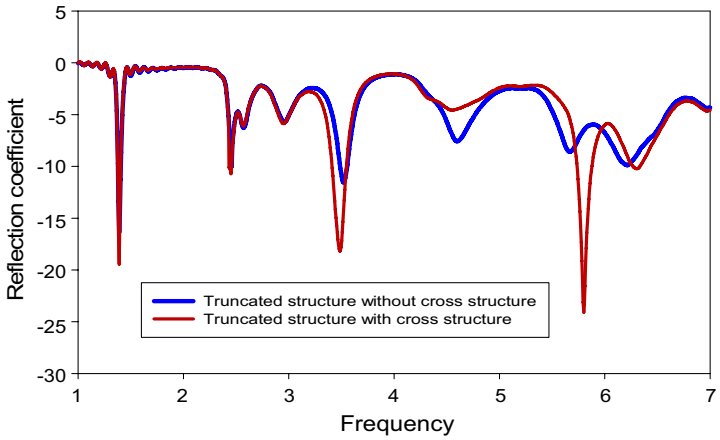

Figure 7. Variation of the reflection coefficient with frequency of proposed antenna with and without the cross structure.

5. RESULTS AND DISCUSSION

A multiband circularly polarized Minkowski fractal slotted truncated patch antenna was fabricated and measured to validate the design. Figure 8 shows the top and bottom views of the fabricated structure of the proposed antenna. The simulated and measured reflection coefficients of the proposed antenna are shown in Figure 9. The simulated results have five resonant frequencies at 1.39 GHz,

(a) (b)

Figure 8. The photograph of the fabricated second iteration Minkowski slotted truncated patch antenna. (a) Front view. (b) Back view.

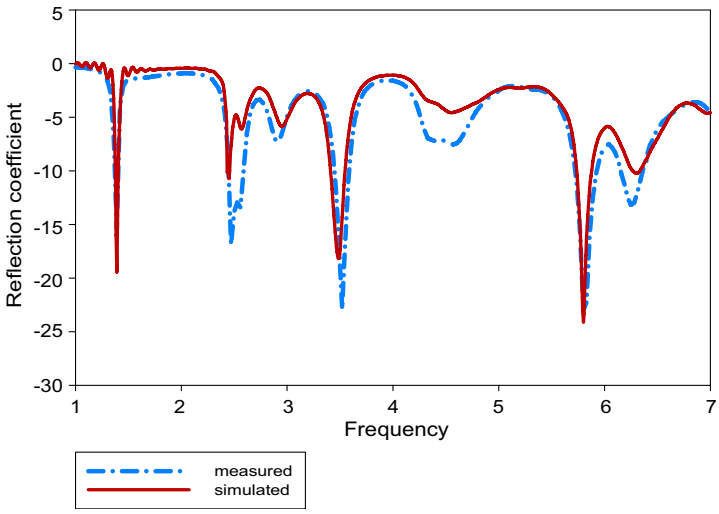

Figure 9. Simulated and measured reflection coefficient with frequency for the proposed antenna.

2.45 GHz, 3.48 GHz, 5.8 GHz, and 6.29 GHz and have reflection coefficients of −19 dB, −11 dB, −18 dB, −24 dB, and −10.2 dB, respectively. The antenna has −10 dB return loss bandwidths of 31 MHz (1.3748 GHz–1.4 GHz), 30 MHz (2.43 GHz–2.46 GHz), 150 MHz (3.4 GHz–3.55 GHz), 210 MHz (5.6 GHz–5.81 GHz), and 78 MHz (6.26 GHz–6.338 GHz) for 1.39 GHz, 2.45 GHz, 3.48 GHz, 5.8 GHz, and 6.29 GHz, respectively. The maximum gain of the antenna is 5.92 dBi for 1.39 GHz, 6.15 dBi for 2.45 GHz, 8.36 dBi for 3.48 GHz, 9.64 dBi for 5.8 GHz, and 6.69 dBi for 6.29 GHz. The measured bandwidth values for the operating frequencies are 30 MHz (1.34 GHz–1.37 GHz) for 1.35 GHz, 124 MHz (2.416 GHz–2.54 GHz) for 2.45 GHz, 150 MHz (3.4 GHz–3.55 GHz) for 3.5 GHz, 20 MHz (5.7 GHz–5.9 GHz) for 5.8 GHz, and 20 MHz (6.15 GHz–6.35 GHz) for 6.25 GHz. Impedance matching is higher in the higher resonant frequency of 5.8 GHz, and therefore, gain is higher at that frequency. Figures 10–14 show simulated and measured radiation patterns of different resonant frequencies.

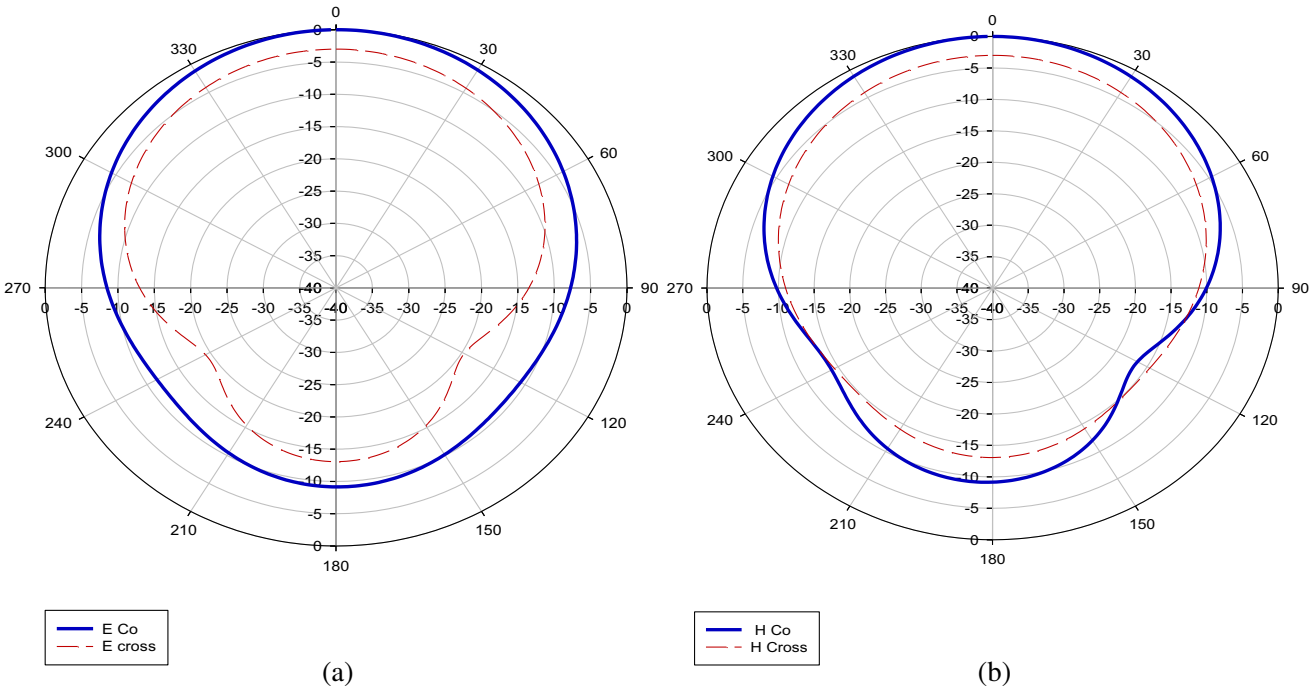

(a) (b)

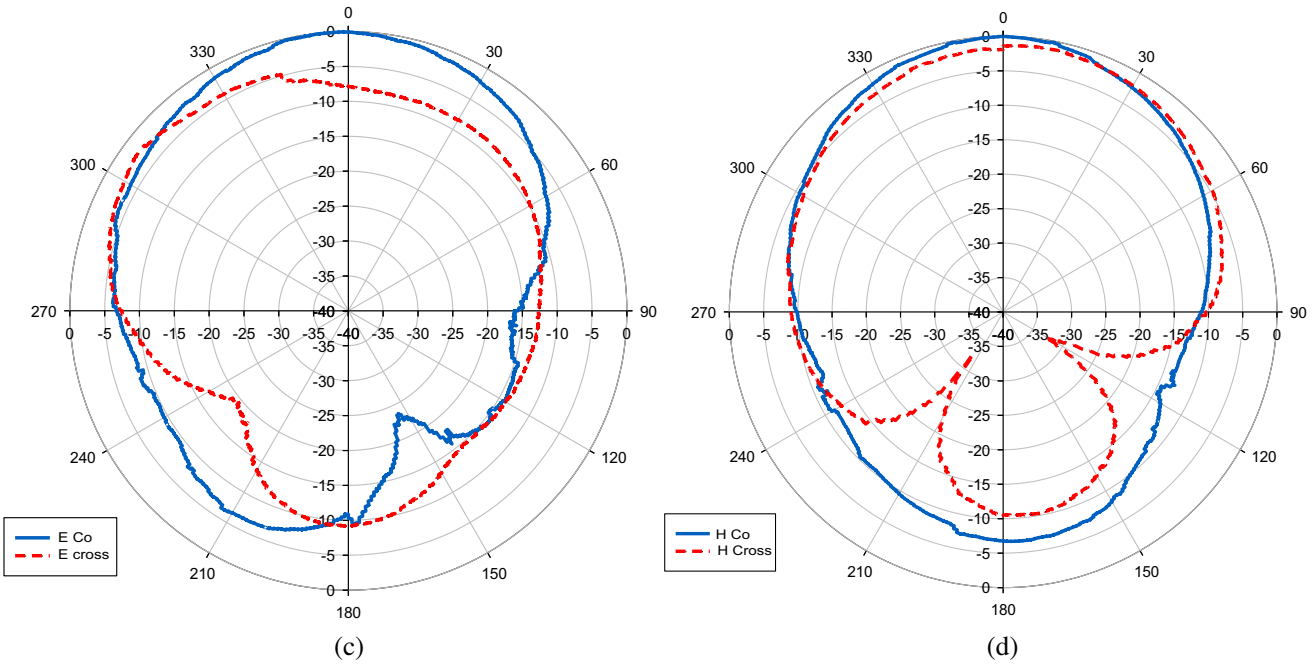

Figure 10. Simulated and measured radiation patterns at 1.37 GHz. (a) Simulated x-z plane. (b) Simulated y-z plane. (c) Measured x-z plane. (d) Measured y-z plane (Co-polarised——blue line and cross polarised– – – – –red line).

The antenna has unidirectional radiation patterns for all the frequency bands. The simulated and measured axial ratio plots at resonant frequency 3.5 GHz of the proposed antenna are shown in Figure 15. The simulated 3 dB axial ratio bandwidth is 3.41 GHz–3.47 GHz, and that of measurement

Table 3. Comparison of the radiation characteristics of the proposed antenna with that in published works.

Design	Patch Dimension	Bandwidth ($S_{11} \leq -10$ dB)	Gain	Axial Ratio bandwidth
Ref. [8]	36 mm × 36 mm	2455–2625 MHz	6 dBi	50 MHz
Ref. [11]	52 mm × 52 mm	2.15–2.71 GHz	2.3 dBi to 3.8 dBi	640 MHz
Ref. [14]	40 mm × 40 mm	2.38–3.03 GHz	2.64 dBi	–
		4.45–5.06 GHz	2.25 dBi	
Ref. [17]	59 mm × 90 mm	1.8–2.82 GHz	2 dBi	–
		4.15–5.95 GHz	3 dBi	–
Ref. [18]	23.4 mm × 32.78 mm	2.40–2.89 GHz	0.35 dB to 3.58 dB	–
		3.40–4.50 GHz		
		5.42–6.18 GHz		
Proposed Antenna	40 mm × 42 mm	1.34 GHz–1.37 GHz	5.92 dBi	–
		2.416 GHz–2.54 GHz	6.15 dBi	
		3.4 GHz–3.55 GHz	8.36 dBi	50 MHz
		5.7 GHz–5.9 GHz	9.64 dBi	–
		6.15 GHz–6.35 GHz	6.69 dBi	

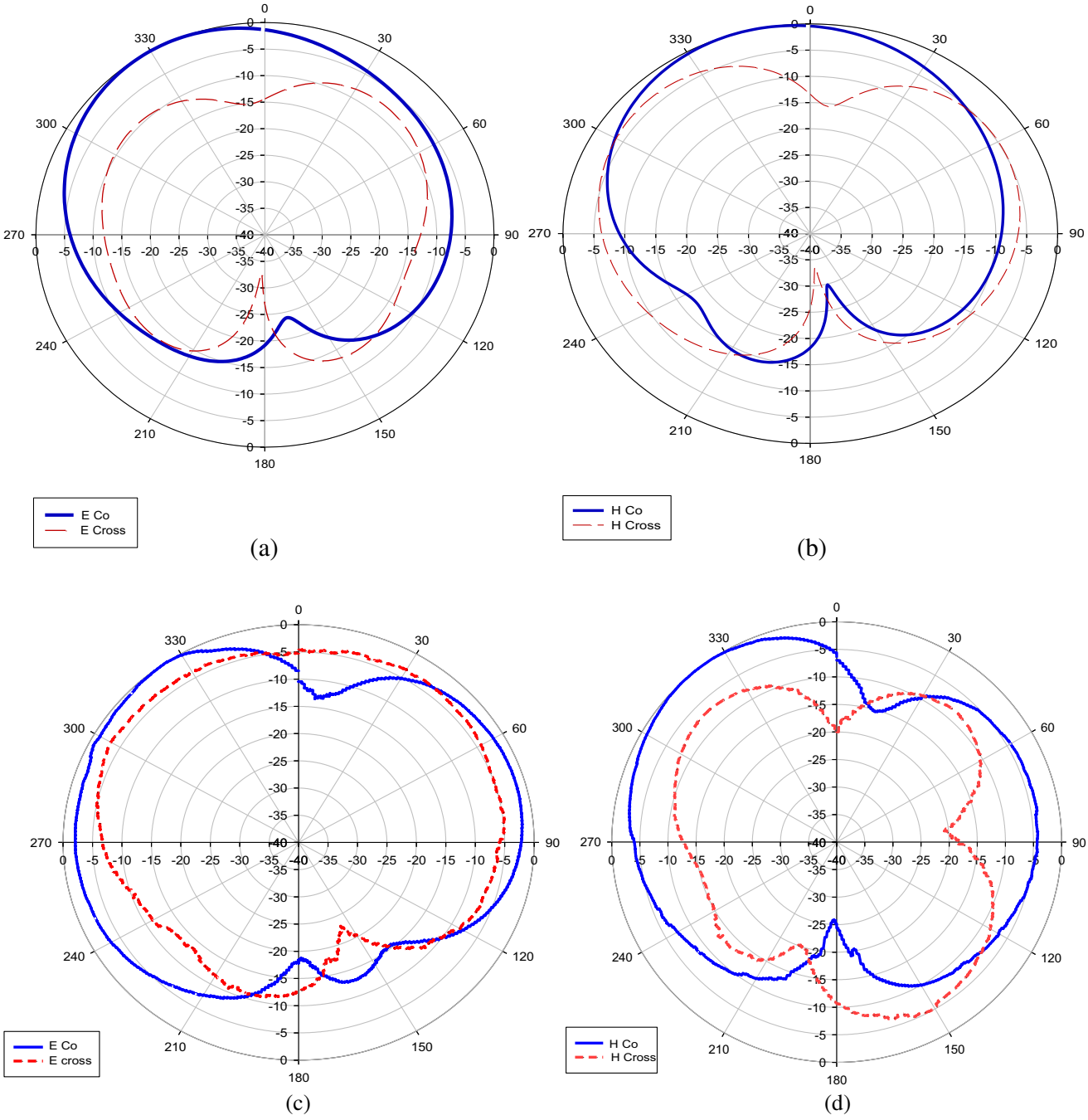

Figure 11. Simulated and measured radiation patterns at 2.44 GHz. (a) Simulated x-z plane. (b) Simulated y-z plane. (c) Measured x-z plane. (d) Measured y-z plane (Co-polarised____blue line and cross polarised– – – – –red line).

is 3.42 GHz–3.47 GHz.

The surface current distributions of the proposed antenna for the five resonant frequencies are shown in Figures 16(a)–(e). From Figures 16(a)–(e), it is shown that modes TM_{11}, TM_{11}, TM_{22}, TM_{33}, and TM_{22} are responsible for the resonant frequencies 1.39 GHz, 2.45 GHz, 3.46 GHz, 5.8 GHz, and 6.29 GHz, respectively.

Resonant mode and current path on the surface of the patch are affected by applying fractal

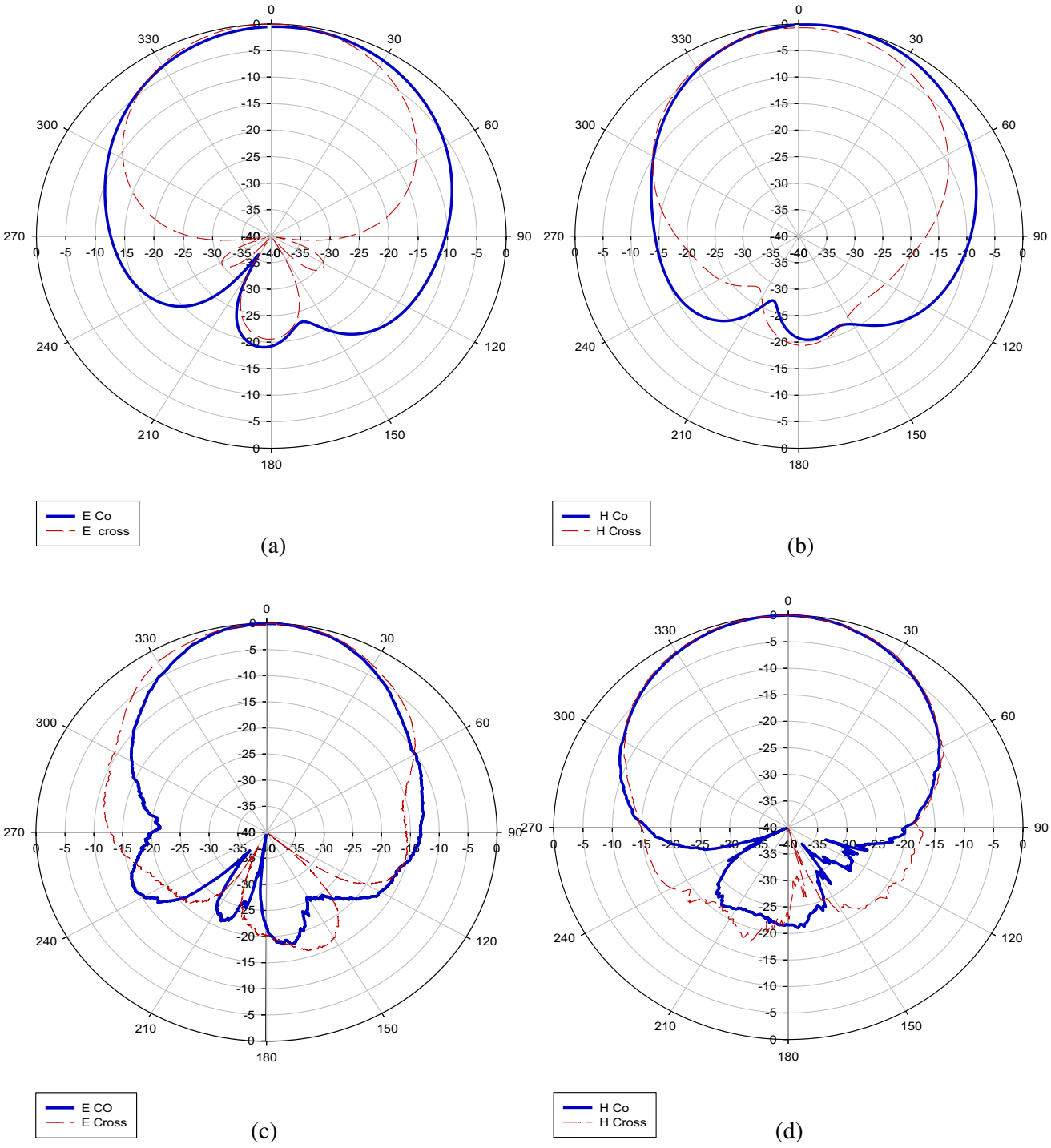

Figure 12. Simulated and measured radiation patterns at 3.46 GHz. (a) Simulated x-z plane. (b) Simulated y-z plane. (c) Measured x-z plane. (d) Measured y-z plane (Co-polarised___blue line and cross polarised– – – – –red line).

geometry on the patch. The simulated surface current distributions on the patch for different phase angles at frequency 3.46 GHz are shown in Figures 17(a) to (d). From the figures, it is clear that the fractal slot area has higher current intensity.

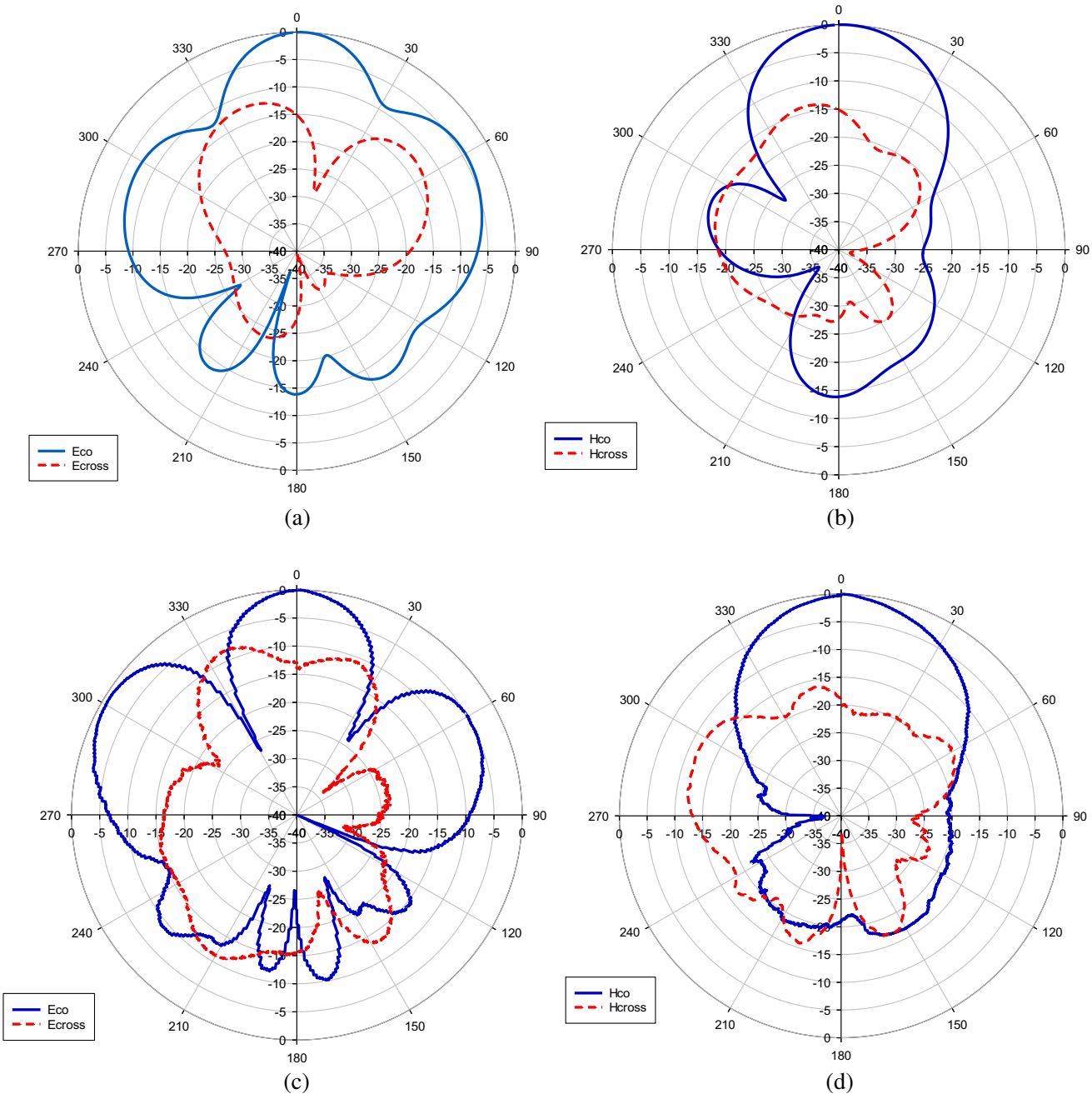

Figure 13. Simulated and measured radiation patterns at 5.7 GHz. (a) Simulated x-z plane. (b) Simulated y-z plane. (c) Measured x-z plane. (d) Measured y-z plane (Co-polarised____blue line and cross polarised– – – – –red line).

The surface current distributions at $\varphi = 0°$ are equal in magnitude and opposite in direction to that at $\varphi = 180°$. Similarly, the surface current distributions at $\varphi = 90°$ and $\varphi = 270°$ are also equal in magnitude and opposite in direction, thereby satisfying the criteria for circular polarization. The direction of rotation of current is anticlockwise, and hence the sense of polarization is left-handed circular polarization.

Table 3 shows the comparison of the radiation characteristics between the proposed antenna and published works by other researchers. It can be observed that the proposed antenna has a superior performance by considering multiband behavior, circular polarization, reflection coefficient, and gain.

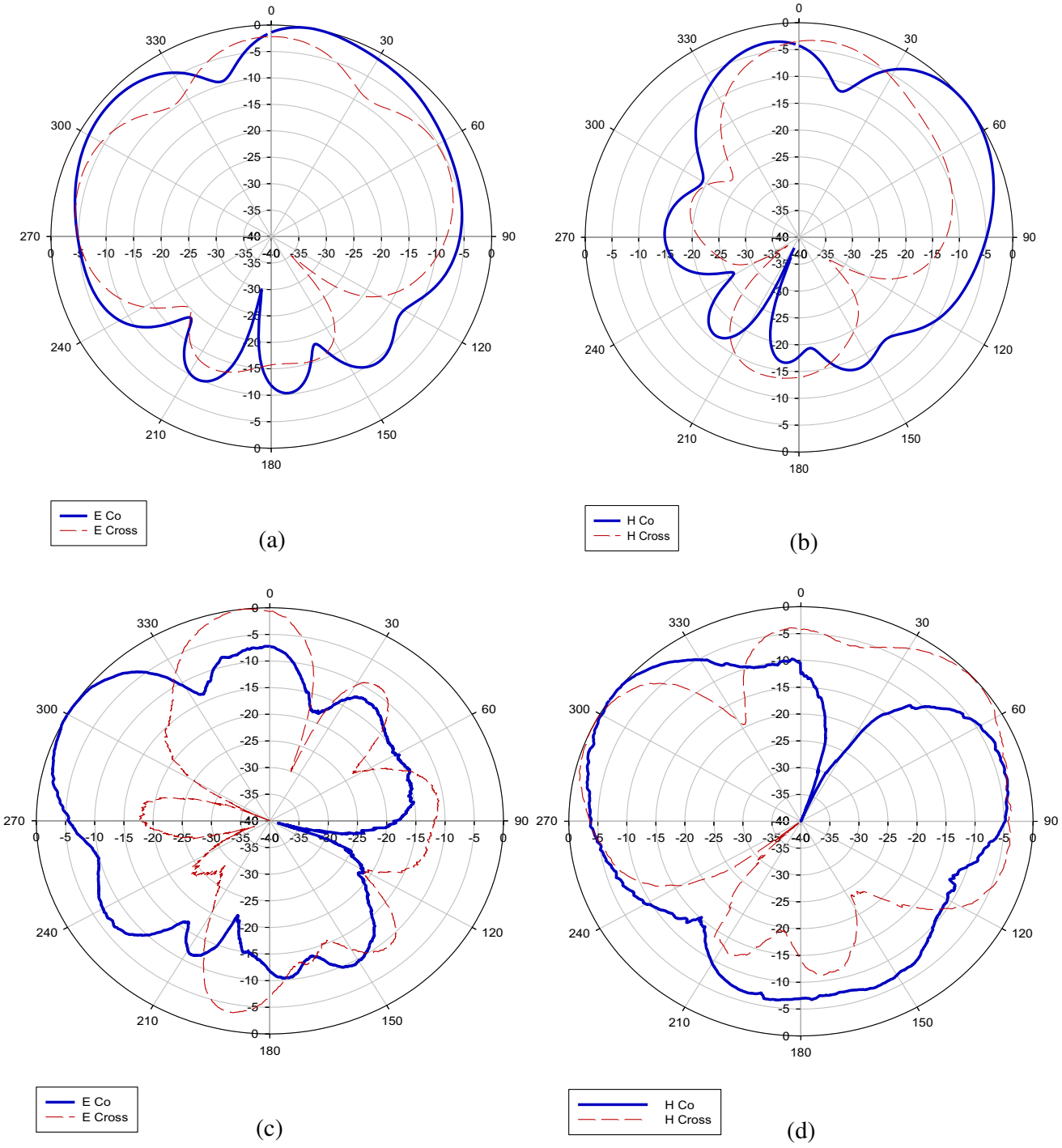

Figure 14. Simulated and measured radiation patterns at 6.27 GHz. (a) Simulated x-z plane. (b) Simulated y-z plane. (c) Measured x-z plane. (d) Measured y-z plane (Co-polarised ___ blue line and cross polarised – – – – – red line).

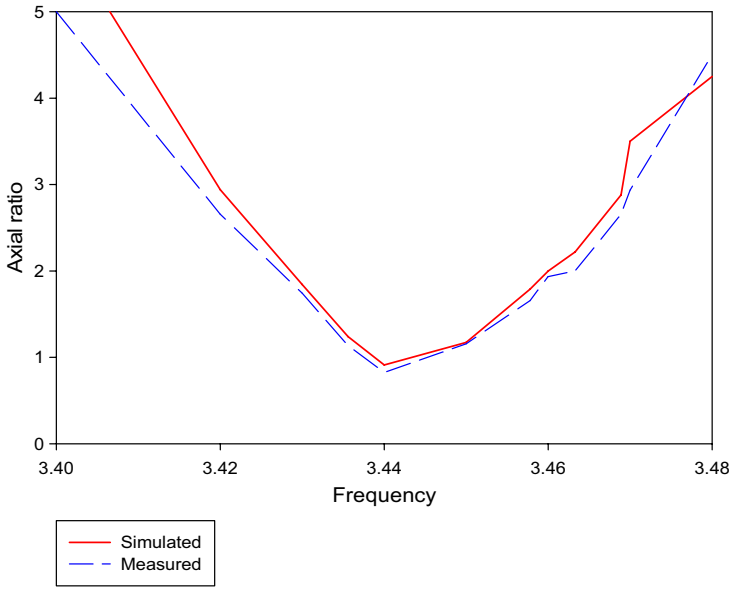

Figure 15. Simulated and measured variations of axial ratio with frequency at the resonant frequency of 3.5 GHz of the proposed antenna.

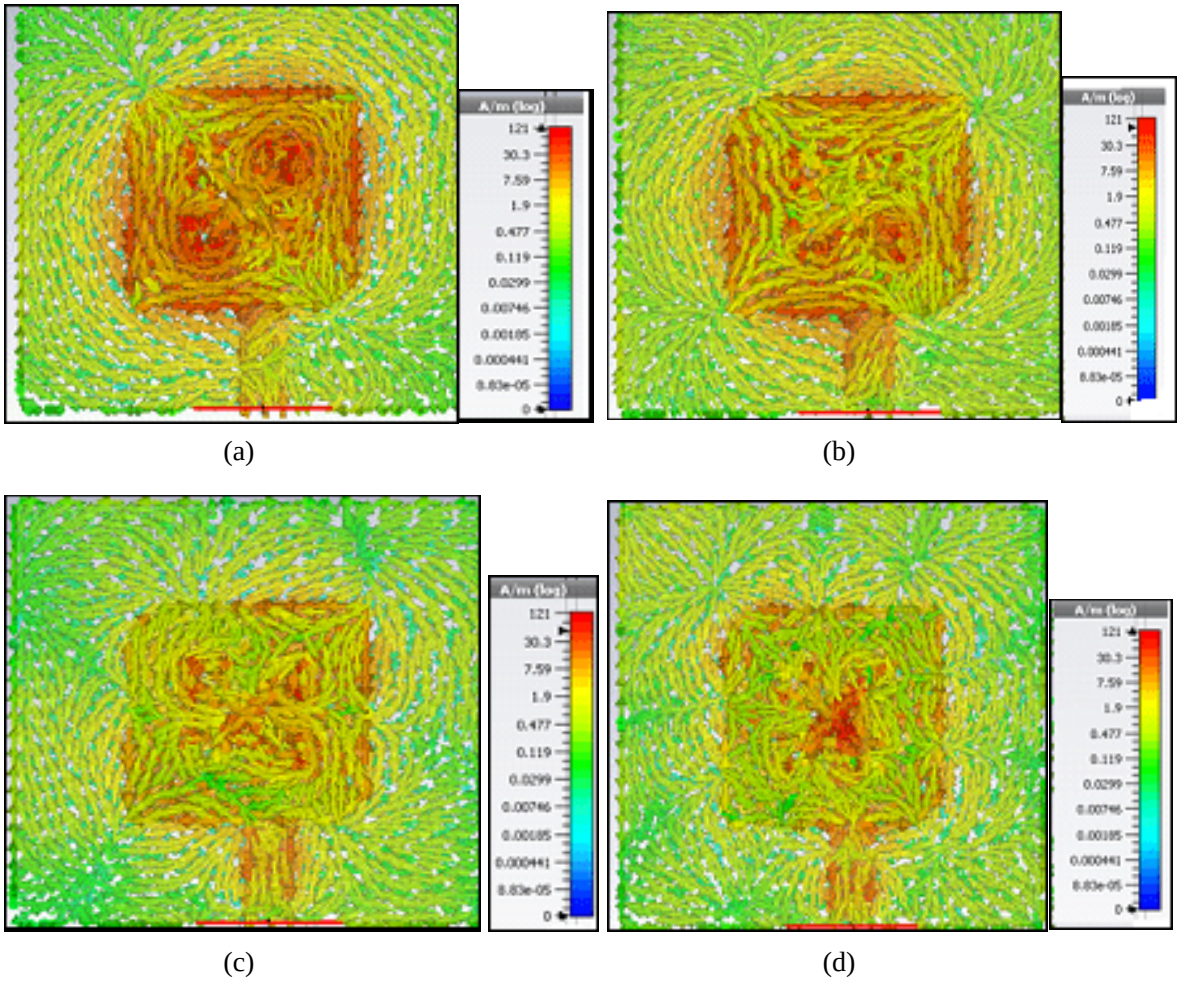

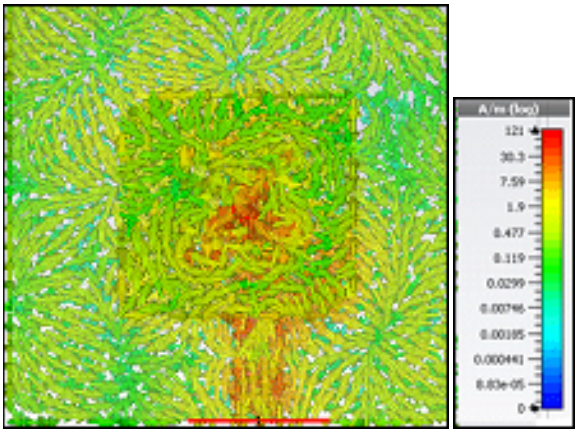

(e)

Figure 16. The surface current distribution of the proposed antenna for the five resonant frequencies. (a) 1.39 GHz, (b) 2.45 GHz, (c) 3.46 GHz, (d) 5.8 GHz, (e) 6.29 GHz.

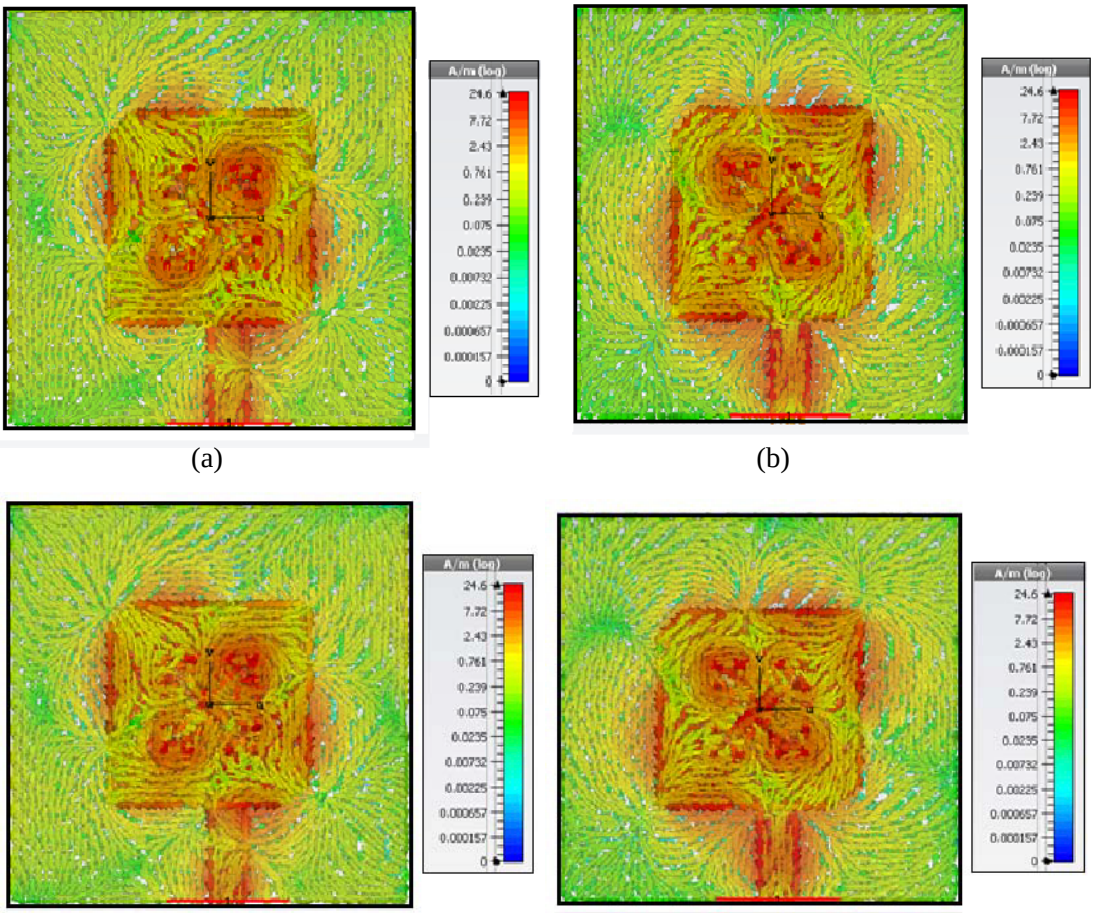

(a) (b)

(c) (d)

Figure 17. Simulated surface current distribution of the antenna at 3.46 GHz for (a) $\varphi = 0°$, (b) $\varphi = 90°$, (c) $\varphi = 180°$, (d) $\varphi = 270°$.

6. CONCLUSION

A multiband circularly polarized Minkowski slotted truncated microstrip patch antenna for wireless application is presented. The antenna supports five resonances at 1.35 GHz, 2.45 GHz, 3.5 GHz, 5.8 GHz, and 6.25 GHz. The optimized antenna has peak gains of 5.9 dBi for 1.35 GHz, 6.15 dBi for 2.45 GHz, 8.36 dBi for 3.5 GHz, 9.64 dBi for 5.8 GHz, and 6.69 dBi for 6. 25 GHz respectively and an axial ratio bandwidth of 50 MHz (3.42 GHz–3.47 GHz). It is compact and provides high gain and circular polarization at one resonant frequency of 3.5 GHz. Hence, it has the potential to be used in wireless communication like Wi-Fi, Wi-Max, and U-NII.

REFERENCES

1. Balanis, A., *Antenna Theory Analysis, and Design*, 3rd Edition, John Wiley and Sons, Hoboken, NJ, 2005.
2. Sim, C. Y. D., "Experimental studies of a shorted triangular microstrip patch antenna embedded with dual V-shaped slots," *Journal of Electromagnetic Waves and Applications*, Vol. 21, No. 1, 15–24, 2007.
3. Krishna, D. D., M. Gopikrishna, C. Aanandan, P. Mohanan, and K. Vasudevan, "Compact dual band slot loaded circular microstrip antenna with a superstrate," *Progress In Electromagnetics Research*, Vol. 83, 245–255, 2008.
4. Das, A., B. Datta, S. Chatterjee, M. Mukherjee, and S. K. Chowdhury, "Dual-band slotted microstrip patch antenna design for application in microwave communication," *International Conference on Information Communication and Embedded Systems (ICICES)*, 2013.
5. Verma, S., J. A. Ansari, and M. K. Verma, "A novel compact multiband microstrip antenna with multiple narrow slits," *Microwave and Optical Technology Letters*, Vol. 55, No. 6, June 2013.
6. Awan, W. A., N. Hussain, S. A. Naqvi, A. Iqbal, R. Striker, D. Mitra, and B. D. Braaten, "A miniaturized wideband and multi-band on-demand reconfigurable antenna for compact and portable devices," *International Journal of Electronics and Communications (AEÜ)*, Vol. 122, 153266, 2020.
7. Iqbal, A., M. A. Selmi, L. F. Abdulrazak, O. A. Saraereh, N. K. Mallat, and A. Smida, "A compact substrate integrated waveguide cavity-backed self-triplexing antenna," *IEEE Transactions on Circuits and Systems II: Express Briefs*, 2020, doi: 10.1109/TCSII.2020.2966527.
8. Reddy, V. V. and N. V. S. N. Sarma, "Compact circularly polarized asymmetrical fractal boundary microstrip antenna for wireless applications," *IEEE Antennas and Wireless Propagation Letters*, Vol. 13, 2014.
9. Chen, W.-S., C.-K. Wu, and K.-L. Wong, "Novel compact circularly polarized square microstrip antenna," *IEEE Transactions on Antennas and Propagation*, Vol. 49, No. 3, March 2001.
10. Albooyeh, M., N. Komjani, and M. Shobeyri, "A novel cross-slot geometry to improve impedance bandwidth of microstrip antennas," *Progress In Electromagnetics Research Letters*, Vol. 4, 63–72, 2008.
11. Chen, L., X. Ren, Y.-Z. Yin, and Z. Wang, "Broadband CPW-fed circularly polarized antenna with an irregular slot for 2.45 GHz RFID reader," *Progress In Electromagnetics Research Letters*, Vol. 41, 77–86, 2013.
12. Yang, L., N.-W. Liu, Z.-Y. Zhang, G. Fu, Q.-Q. Liu, and S. Zuo, "A novel single feed omnidirectional circularly polarized antenna with wide AR bandwidth," *Progress In Electromagnetics Research C*, Vol. 51, 35–43, 2014.
13. Bhatia, S. S. and N. Sharma, "A compact wideband antenna using partial ground plane with truncated corners, L-shaped stubs and inverted T-shaped slots," *Progress In Electromagnetics Research M*, Vol. 97, 133–144, 2020.
14. Yassen, M. T., M. R. Hussan, H. A. Hammas, H. Al-Saedi, and J. K. Ali, "A compact dual-band slot antenna based on Koch fractal Snowflake annular ring," *2017 Progress In Electromagnetics Research Symposium — Spring (PIERS)*, 670–674, St Petersburg, Russia, May 22–25, 2017.

15. Ali, J. K. and E. S. Ahmed, "A new fractal based printed slot antenna for dual band wireless communication applications," *Progress In Electromagnetics Research Symposium Proceedings*, 1507–1510, Kuala Lumpur, Malaysia, March 27–30, 2012.
16. Abdul Karim, S. F., A. J. Salim, J. K. Ali, A. I. Hammoodi, M. T. Yassen, and M. R. Hassan, "A compact Peano-type fractal-based printed slot antenna for dual-band wireless applications," *2013 IEEE International RF and Microwave Conference, RFM 2013*, Penang, Malaysia, 2013.
17. Mahatthanajatuphat, C., S. Saleekaw, P. Akkaraekthalin, and M. Krairiksh, "A rhombic patch monopole antenna with modified Minkowski fractal geometry for Umts, WLAN, and mobile WiMAX application," *Progress In Electromagnetics Research*, Vol. 89, 57–74, 2009.
18. Ali, J. K., M. T. Yassen, M. R. Hassan, and A. J. Salim, "A printed fractal-based slot antenna for multi-band wireless communication applications," *PIERS Proceedings*, 613–617, Moscow, Russia, August 19–23, 2012.
19. Kordzadeh, A. and F. Hojat Kashani, "A new reduced size microstrip patch antenna with fractal shaped defects," *Progress In Electromagnetics Research B*, Vol. 11, 29–37, 2009.
20. Heydari, S., P. Jahangiri, A. S. Arezoomand, and F. B. Zarrabi, "Circular polarization fractal slot by jerusalem cross slot for wireless applications," *Progress In Electromagnetics Research Letters*, Vol. 63, 79–84, 2016.
21. Ali, J. K., Z. A. Abed Al-Hussain, A. A. Osman, and A. J. Salim, "A new compact size fractal based microstrip slot antenna for GPS applications," *PIERS Proceedings*, 705–708, Kuala Lumpur, Malaysia, March 27–30, 2012.
22. Mukti, P. H., S. H. Wibowo, and E. Setijad, "A compact wideband fractal-based planar antenna with meandered transmission line for L-band applications," *Progress In Electromagnetics Research C*, Vol. 61, 139–147, 2016.
23. Mandelbrot, B. B., *The Fractal Geometry of Nature*, W. H. Freeman, San Francisco, CA, 1982.
24. Ataeiseresht, R., Ch. Ghobadi, and J. Nourinia, "A novel analysis of Minkowski fractal microstrip patch antenna," *Journal of Electromagnetic Waves and Applications*, Vol. 20, No. 8, 1115–1127, 2006.
25. Borja, C. and J. Romeu, "Multiband Sierpinski fractal patch antenna," *IEEE International Symposium on Antennas and Propagation Digest*, Vol. 3, 1708–1711, Salt Lake City, Utah, July 2000.